

Design of temperature insensitive *in vivo* strain sensor using multilayer single mode optical fiber

F. MAKOU EI, S. MAKOU EI (✉)

Faculty of Electrical and Computer Engineering, University of Tabriz, Tabriz 51664, Iran

© Higher Education Press and Springer-Verlag Berlin Heidelberg 2016

Abstract Bone strain measurement is a case of interest and demanding task for osteogenic adaption responses. In this paper, a novel biocompatible optical sensor for the bone axial strain measurement was proposed. In case modern multilayer single mode WII type optical fibers are well designed, they exhibit superior characteristics compared to conventional metal strain gauges (SGs). Furthermore, they could be strong competitors for SGs based on fiber Bragg grating (FBG) devices. In this study, mode field diameter (MFD) was selected as the indirect parameter for sensing task, which was totally a new approach. The strain sensitivity of $70.7733 \text{ pm}/\mu\epsilon$ was obtained. Moreover, temperature sensitivity was $-3.0031 \times 10^{-6} \text{ pm}/^\circ\text{C}$, which was negligible and removed the temperature compensation complexity for the sensor structure presented. The satisfactory property achieved for the designed sensor is as a result of multilayer fiber's complicated structure as well as the design procedure based on evolutionary genetic algorithm (GA). In addition, the sensor demonstrated a reliable performance as its sensitivity was independent of the magnitude of the applied load.

Keywords bone strain, *in vivo*, optical strain gauge (SG), genetic algorithm (GA)

1 Introduction

The primary function of bone is to support the body, provide a mechanical basis for movement, protect vital organs as well as prevent the excessive deformation of surrounding tissues under external forces [1]. During the past decades, scientists have been trying to describe the relationship between bone strain and bone osteogenic

responses quantitatively [2]. Bone adapts its structure to mechanical loading. It is essential to understand the form and function of the skeleton, the quantification of the experienced strain and the loading. The gold standard for strain measurement is often obtained by strain gauge (SG), a device with electrical resistance varying in proportion to the amount of strain. However, it faces some serious drawbacks for operation *in vivo*. Mostly because it is difficult to adhere to bone, the SG itself with its measurement wires represents a substantial foreign body implant [3].

Less invasive and more accurate way to reveal strain effect, thus improving the understanding of bone strain within the human has become a hot topic in the field of bone research. The revolutions in the fiber optic technology have enabled the development of fiber optic sensors (FOSs). FOSs, as dielectric devices, have a number of advantages over their electrical counterparts for operation in human body, and they are the primary candidates for complete sensing systems. Their desirable characteristics include biocompatibility, easier adherence to bone, corrosion resistance, and insensitivity to electromagnetic interferences [4]. Also, the smaller size and surface area of smooth optic fibers compared to SG with many soldered seams are profitable not only because they probably represent a smaller risk of infection when used *in vivo*, but also because they can be used on curved surfaces which is a problem with SG [3].

Among the FOSs, fiber Bragg grating (FBG) strain sensors have undergone a rapid development in the recent years and have been widely investigated. It has been reported that the sensitivity for strain and temperature of a FBG recorded at 1550 nm are approximately $1.2 \text{ pm}/\mu\epsilon$ and $13.7 \text{ pm}/^\circ\text{C}$ [4,5]. For *in vivo* measurements when strain values are only required, cross sensitivity of FBG to temperature must be taken into account, and it will be compensated with accurate implementation techniques [6], instead of assuming these effects negligible under apparently controlled situations. *In vivo* applications

under infectious process or vigorous physical activity, which are always followed by an increase in temperature, or in long-term monitoring temperature corrections must be made [4]. Also, some researchers have introduced a sensor scheme consisting of combination of a polymer FBG and a silica FBG which gives large discrimination against temperature and strain and provides large sensitivity and dynamic range for sensing temperature and strain changes simultaneously and independently [7]. However, to the best of our knowledge, the viability of this sensor for *in vivo* use is not inspected.

Modern multilayer optical fibers for strain sensing by a precise targeted design were presented, and they might become strong competitors due to their lower temperature sensitivity and satisfactory strain response. The variety in the hyper-parameters of these fibers and distinct affections of these parameters make the utilization of an optimization tool essential for permissible response of the designed fiber. The evolutionary genetic algorithm (GA) [8,9] is the best choice for the specific conditions of this case. In this paper, the effect of strain on refractive index through the mode field diameter (MFD) of the multilayer single mode WII type optical fiber and the potential of this fiber as a strain sensor were explored.

This paper is organized as follows: Section 2, being the mathematical formulation, contains the prerequisite information about modal analysis, strain, and thermal effect on optical fiber. In Section 3, using GA and considering the specific conditions *in vivo*, a suitable structure was proposed for the fiber. In the following section, the simulation and calculated results as well as discussion are exhibited and finally the conclusion is presented.

2 Mathematical formulation

The mathematical formulation to extract the required relations for simulation and design are illustrated in this section. Three distinct subsections are allocated to the factors playing role in the sensor design and the sensor behavior identification.

2.1 Modal analysis

In this subsection, we presented modal analysis based on linear polarized (LP) approximation for the WII type triple

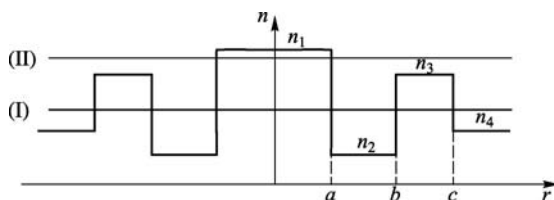


Fig. 1 Index of refraction profile for the proposed structures (WII)

clad single mode optical fiber illustrated in Fig. 1 [10].

For this structure, the index of refraction is defined as follows:

$$n(r) = \begin{cases} n_1, & 0 < r < a, \\ n_2, & a < r < b, \\ n_3, & b < r < c, \\ n_4, & c < r, \end{cases} \quad (1)$$

where r is the radius position of the optical fiber. According to LP approximation [11,12], we calculated the electrical field distribution through the solution of Maxwell's equations. There are two regions of operation, and guided modes and propagating wave vectors can be obtained by using two determinants which were constructed by boundary conditions. The two gray transverse lines in Fig. 1 demonstrate these two operation regions. The effective refractive index is given by

$$n_{\text{eff}} = \frac{\beta_g}{k_0}, \quad (2)$$

where β_g is the longitudinal propagation constant of the guided mode and k_0 is the wave number in vacuum. Structural parameters are defined as follows.

$$R_1 = \frac{n_1 - n_3}{n_3 - n_2}, R_2 = \frac{n_2 - n_4}{n_3 - n_2}, \Delta = \frac{n_1^2 - n_4^2}{2n_4^2} \approx \frac{n_1 - n_4}{n_4},$$

$$P = \frac{b}{c}, Q = \frac{a}{c}. \quad (3)$$

Since the field of the fundamental mode of a circularly symmetric fiber is bell shaped and has circular symmetry, its extent could be well described by a single parameter, which defines the MFD [13].

$$\text{MFD}^2 = 8 \frac{\int_0^\infty |\psi(r)|^2 r dr}{\int_0^\infty \left| \frac{d\psi(r)}{dr} \right|^2 r dr}, \quad (4)$$

where $\psi(r)$ is modal field distribution.

2.2 Strain effect

Strain is the geometric deformation within the material, and it can be expressed as the ratio between the change of length and original length, therefore it is given a dimensionless number. Strain can be simply tensile or compressive. More complex strains are generated by two planes sliding over each other (shear strain), bending (bending strain) or rotation (torsion strain). Axial strain in Fig. 2 [2] is a strain in the same direction as the applied load. Both compressive strain and tensile strain, with

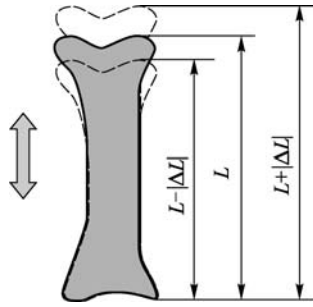


Fig. 2 Axial bone strain

negative and positive values, respectively, are axial strains. For long bones, axial strain under physiologic conditions is mostly along the long axis of the bone. It is generally thought that compressive and tensile strains are the main component for most kinds of activities [2].

Having the feasibility of strain measurement in bones, diverse bone parameters could be accomplished. Pressure mapping and the assessment of contact force and stresses would be provided using an embedded array of optical sensors. Strain measurement in the fractured area of bone after surgery and at the bone joints for rehabilitation purposes is of great prominence. Moreover, the strain response gives a direct indication of the degree of calcium in the bone. Calcium is the most important mineral in body and decalcification can change the mechanical integrity of the bones [14].

A modern multilayer optical fiber response to strain occurs due to both changes in the refractive index and dimensions of the layer which manage the n_{eff} variation. The term relating the refractive index changing with strain is dominated by photoelastic effect. Getting exposed to strain, the bandgap shift of silica causes the change in the absorption coefficient of it. According to the Kramers-Kronig relation, the variation in the absorption coefficient affects the refractive index of silica. Therefore, the strain-induced bandgap change is related to the changes of the refractive index [15,16].

Physical changes in core height and width are related to the Poisson ratio (ν). However, the contributions of these has been calculated to be negligible in our study.

Generally, considering the thermal induced strain due to temperature variation, the change in refractive index as a result of strain can be deduced as follows [10]

$$\Delta n_i = \sum_{i,j=1}^6 \frac{\partial n_i}{\partial \varepsilon_j} \varepsilon_j + \frac{\partial n_i}{\partial T} \Delta T = -\frac{n_i^3}{2} \sum_{i,j=1}^6 p_{ij} \varepsilon_j + \frac{\partial n_i}{\partial T} \Delta T, \quad (5)$$

where p_{ij} is the photoelastic coefficient, n_i is the refractive index of the i th layer, ε_j is the strain tensor element and ΔT is the temperature variation.

Assuming the homogeneity and isotropic behavior of silica and also the application of force perpendicular to the fiber cross section, Eq. (5) can be simplified to

$$\Delta n_i = -\frac{n_i^3}{2} (p_{12} - \nu(p_{11} + p_{12})) \varepsilon + \frac{\partial n_i}{\partial T} \Delta T, \quad (6)$$

where, for the pure silica, $p_{11} = 0.113$, $p_{12} = 0.252$, $\nu = 0.17$.

2.3 Temperature effect

It is well understood that the refractive index of silica varies with the change of temperature. As a result, generally real time compensation to the temperature fluctuation is on demand in applications. The method used in this paper has been introduced by Ghosh [17]. This model is based on the subscription of both electrons and optical phonons. The optical constants computed through this model are then used to calculate the refractive indexes at any operating temperature or wavelength for the optical fiber transmission system. Thermo-optic coefficient dn/dT contains the contribution of electrons and optical phonons. Consequently, it can be described in the optical transmission range in terms of linear expansion coefficient α and the temperature variation of energy gap (dE_g/dT) by the following relation [18]

$$2n(dn/dT) = X_e \left[-3\alpha - \frac{2}{E_g} \frac{dE_g}{dT} \frac{E_g^2}{(E_g^2 - E^2)} \right], \quad (7)$$

where n , X_e , E , and E_g are the room temperature refractive index, the electronic susceptibility, photon energy, and the suitable energy gap lying in the vacuum ultraviolet region, respectively. The above equation can be rewritten in terms of a normalized wavelength $R = \lambda^2 / (\lambda^2 - \lambda_g^2)$ as

$$2n \left(\frac{dn}{dT} \right) = GR + HR^2, \quad (8)$$

where the constants G and H are related respectively to the thermal expansion coefficient (α) and the energy gap temperature coefficient (dE_g/dT) according to the relations presented in Ref. [17] and their values were given in Table 1 for silica glasses.

Table 1 Interpolated coefficient in the relation of Eq. (8)

$G/(\text{ }^\circ)$	$H/(\text{ }^\circ)$	$\lambda_g/\mu\text{m}$	$\alpha/(\text{ }^\circ)$
-1.6548×10^{-6}	31.7794×10^{-6}	0.109	0.45×10^{-6}

3 Design technique of strain sensor using GA

In this section, a design methodology for WII single mode optical fiber is applied to obtain the best performance in the case of MFD sensitivity to the strain. As mentioned in the introduction, the chief target is to maximize ΔMFD as the sensor sensitivity. An appropriate optimization tool is prerequisite for management of all the conditions. The

design technique is based on GA, because this optimization tool has been proven to be effective in nonlinear cases with domains which are too large to be scanned efficiently and also there are plenty of parameters which carry direct impact on result [8,9]. The main target is the maximization of MFD alterations due to strain. If the optical fiber is used as a sensing element and the MFD variation is determined to be an indirect parameter proportional to the strain, it would boost the sensor sensitivity. According to the data table represented in Ref. [2], the strain magnitude in osteogenic structure of body in some vigorous activities can reach approximately $9000 \mu\epsilon$. The MFD is calculated in the well-known wavelength of 1550 nm since silica has the smallest natural attenuation at this wavelength.

To derive the proposed design methodology, the following cost function is introduced,

$$\text{cost function} = \text{MFD}|_{-9000 \mu\epsilon} - \text{MFD}|_{+9000 \mu\epsilon}. \quad (9)$$

The sensitivity of MFD to strain augments as the considered cost function is used. The flowchart given in Fig. 3 explains the design procedure based on evolutionary GA.

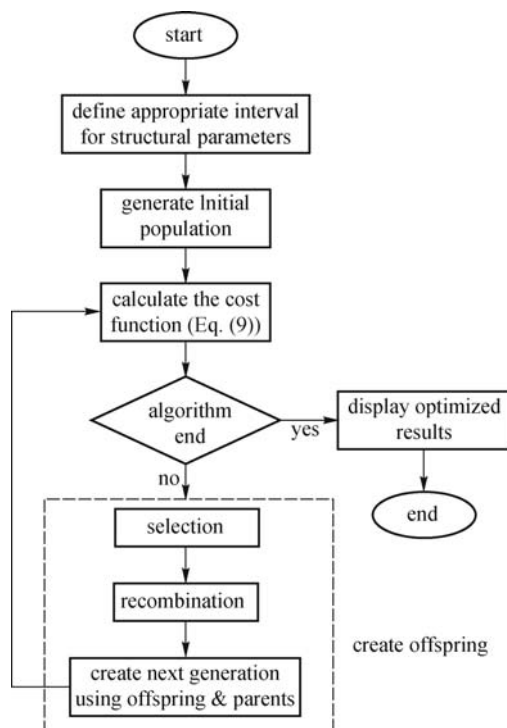


Fig. 3 Scheme of design procedure based on GA

4 Simulation results and discussion

Based on the developed cost function, the simulation results are presented in this section. All simulations are accomplished at $\lambda = 1550 \text{ nm}$ and the designed fiber structure is single mode. The effect of strain on ΔMFD as

the sensor sensitivity is examined in two distinct states: the strain impact in the absence of temperature fluctuations and simultaneous effects of both strain and temperature changes.

A variation of the refractive index or structural parameters of the optical fiber, caused by strain and temperature change, induce a shift of the MFD. The MFD change can be modeled by the following equation

$$\Delta\text{MFD} = S_{\text{strain}}\Delta\epsilon + S_T\Delta T, \quad (10)$$

where S_{strain} and S_T are the strain and temperature sensitivities respectively, $\Delta\epsilon$ and ΔT are the strain and temperature variations respectively. Equation (10) highlights the temperature dependence of strain measurement. In a multilayer optical fiber, the induced strain due to application of external axial force and the strain caused by temperature fluctuations are not independent. Figure 4 shows the response of MFD variation of the fiber structure with the proposed design due to strain. The range of $[-9000 + 9000] \mu\epsilon$ in this graph covers both compressive and tensile strains. Conforming the figure exhibited, it is obvious that generally MFD increases gradually as the applied compressive strain diminishes and then changes to the tensile type. In other words, expansion in compressive and tensile strains lead to contrast effects on MFD and yield reduction and boost, respectively. Through the physical point of view, based on Eq. (6) for compressive strain ($\epsilon < 0$) not only is the refractive index variation due to strain positive but also it has a direct relationship with the layer refractive index value. So, the difference in the core and the first cladding layer refractive indexes grows and thus the light is restricted in the core more than before. This phenomenon generally reduces the MFD. On the other hand, for the tensile strain ($\epsilon > 0$) the difference in the core and the first cladding layer refractive indexes falls. Hence, the fiber capability to bind the light reduces and the electrical field spreads more in the cladding region. In other respects, the field distribution becomes smoother and consequently the MFD enlarges.

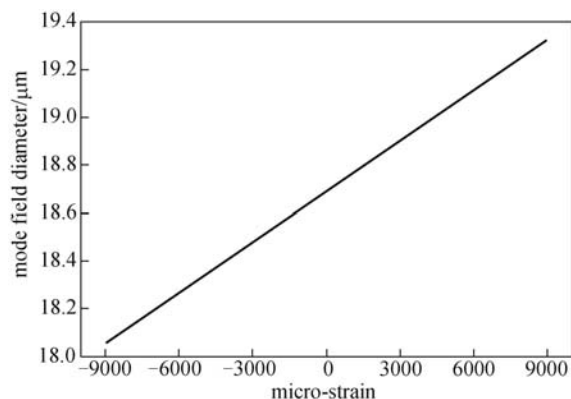


Fig. 4 MFD vs. compressive (–) and tensile (+) strain

Table 2 GA results for optimal values of geometrical and optical parameters

parameter	<i>a</i>	<i>P</i>	<i>Q</i>	Δ	<i>R</i> ₁	<i>R</i> ₂
optimum value	2.2462 μ m	0.70788	0.2950	0.00455	1.339	-0.721

This curve can be represented mathematically by

$$MFD = 18.6645 \times (1 + 3.8917 \times 10^{-6}\epsilon). \quad (11)$$

The strain sensitivity of MFD was 70.7733 pm/ $\mu\epsilon$. Compared to the sensitivity of approximately 1.2 pm/ $\mu\epsilon$ of FBG strain sensors [5], the attained result is far better thanks to the alteration in the nature of indirect parameter chosen for the sensor, which is ΔMFD . To have a meaningful determination of the actual strain, it is necessary to consider the temperature alterations of the body, either. Thus, a specific procedure is taken into account where the strain effect is determined to be the main parameter and the thermal effect is in secondary consideration. Through the interpolation of the attained outcomes, the results are mathematically presented by the following relation

$$\Delta MFD = 70.7733\Delta\epsilon - 3.0031 \times 10^{-6}\Delta T. \quad (12)$$

Here, -3.0031×10^{-6} pm/ $^{\circ}C$ is the temperature sensitivity of the sensor. The attained results indicate the linear effect of temperature on ΔMFD for different applied strains. The temperature changes in the measurement of the strain has a reduction impact. In other words, ΔMFD evaluated in the absence of thermal effect has a higher value than the one without temperature variations.

The attained result indicates that the designed optical strain sensor is approximately insensitive to the temperature changes in body and hence the complexity of temperature compensation is whisked away. Note that, the represented explanations are for the specific fiber structure designed for strain sensing purpose. The outputs attained from optimization process are presented in Table 2.

For better clarification the temperature insensitivity of the designed strain sensor for *in vivo* applications, Fig. 5 is presented. According to this figure, it is obvious that the MFD experiences almost no variation due to temperature variation. On the other hand, the changes in MFD due to strain is evident.

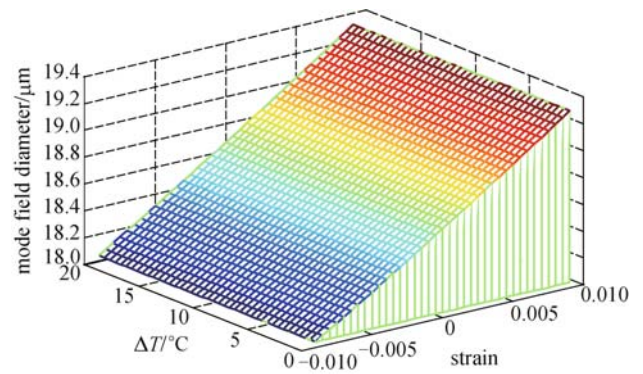


Fig. 5 MFD vs. strain and temperature

An important concept to consider for a sensor being employed is its reliability. Admittedly, the strain magnitude affects the sensitivity in a strain sensor. Therefore, in the second part of this section, it was investigated whether the different strain magnitudes lead to distinct sensitivities in the proposed fiber optic sensor. To do so, neglecting the thermal effect, S_{strain} for a range of various maximum strains in the system was simulated, and the results were shown in Fig. 6. According to the simulation results, there is a semi-linear trend for sensor sensitivity-strain curve. Although for lower strain levels the sensitivity of the

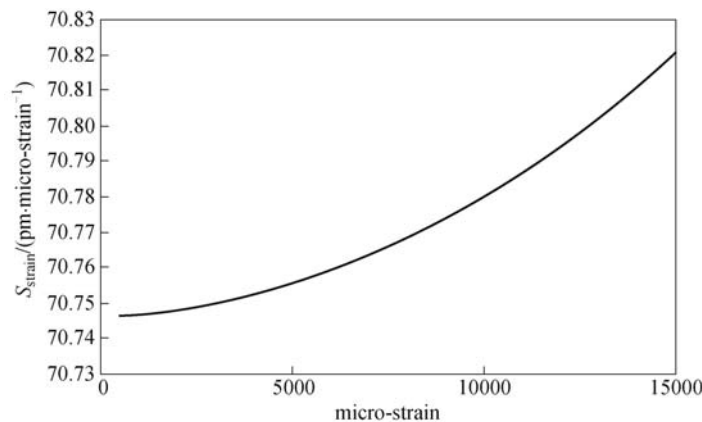


Fig. 6 Sensor sensitivity vs. applied strain

sensor was reduced, this decrement was not remarkable, which confirms the reliability of this sensor.

5 Conclusions

In this paper, a strain sensor by the means of WII type single mode optical fiber was designed, in which the indirect parameter for strain measurement was the MFD. The evolutionary GA was utilized in the design process. The simulation results admitted the temperature insensitivity of the designed structure for *in vivo* strain measurement. The evaluated value for temperature sensitivity was -3.0031×10^{-6} pm/°C. Thus, the temperature compensation techniques was not required in the proposed fiber structure, which leads to the simplification of its use. In addition, the obtained strain sensitivity was 70.7733 pm/με. Although the character of the indirect parameter employed in this work was different from FBGs, compared to them with the strain sensitivity of approximately 1.2 pm/με, higher sensitivity was obtained in this paper. As a result, more precise monitoring of smaller experienced strains in body is possible. The other feature of this designed sensors was the almost linear relation of sensor sensitivity and the induced strain. In other words, the sensor behavior for the range of loadings in human body was resistant.

References

1. Bekker A, Cloete T J, Chinsamy-Turan A, Nurick G N, Kok S. Constant strain rate compression of bovine cortical bone on the Split-Hopkinson Pressure Bar. *Materials Science and Engineering C*, 2015, 46: 443–449
2. Yang P F, Brüggemann G P, Rittweger J. What do we currently know from *in vivo* bone strain measurements in humans? *Musculoskeletal & Neuronal Interact*, 2011, 11(1): 8–20
3. Fresvig T, Ludvigsen P, Steen H, Reikerås O. Fibre optic Bragg grating sensors: an alternative method to strain gauges for measuring deformation in bone. *Medical Engineering & Physics*, 2008, 30(1): 104–108
4. Roriz P, Carvalho L, Frazão O, Santos J L, Simões J A. From conventional sensors to fibre optic sensors for strain and force measurements in biomechanics applications: a review. *Journal of Biomechanics*, 2014, 47(6): 1251–1261
5. Othonos A. Fiber Bragg gratings. *Journal of Scientific Instruments*, 1997, 68(12): 4309–4341
6. Reekie L, Dakin J P, Archambault J L, Xu M G. Discrimination between strain and temperature effects using dual-wavelength fiber grating sensors. *Electronics Letters*, 1994, 30(13): 1085–1087
7. Liu H B, Liu H Y, Peng G D, Chu P L. Strain and temperature sensor using a combination of polymer and silica fibre Bragg gratings. *Optics Communications*, 2003, 219(1-6): 139–142
8. Holland J H. *Adaptation in Natural and Artificial Systems*. 4th ed. Cambridge, MA: MIT Press, 1992
9. Goldberg D E. *Genetic Algorithms in Search, Optimization and Machine Learning*. New York: Addison-Wesley, 1989
10. Zhang X, Tian X. Analyzes of waveguide dispersion characteristics of WI- and WII-type triple-clad single-mode fibers. *Optics & Laser Technology*, 2003, 35(4): 237–244
11. Makouei S, Oskouei M S, Rostami A. Study of bending loss and mode field diameter in depressed inner core triple clad single mode optical fibers. *Optics Communications*, 2007, 280(1): 58–67
12. Gatak A, Thyagarajan K. *Introduction to Fiber Optics*. 3rd ed. Cambridge: Cambridge University Press, 2002
13. Artiglia M, Coppa G, Di Vita P, Potenza M, Sharma A. Mode field diameter measurements in single mode optical fibers. *IEEE Journal of Lightwave Technology*, 1989, 7(8): 1139–1152
14. Mishra V, Singh N, Rai D V, Tiwari U, Poddar G C, Jain S C, Mondal S K, Kapur P. Fiber Bragg grating sensor for monitoring bone decalcification. *Orthopaedics & Traumatology, Surgery & Research*, 2010, 96(6): 646–651
15. Mignani A G, Baldini F. Biomedical sensors using optical fibres. *Reports on Progress in Physics*, 1996, 59(1): 1–28
16. Cai J, Ishikawa Y, Wada K. Strain induced bandgap and refractive index variation of silicon. *Optics Express*, 2013, 21(6): 7162–7170
17. Ghosh G. Temperature dispersion of refractive indexes in some silicate fiber glasses. *Photonics Technology Letters*, 1994, 6(3): 431–433
18. Ghosh G. Dispersion of temperature coefficients of birefringence in some chalcopyrite crystals. *Applied Optics*, 1984, 23(7): 976–978



F. Makouei received her B.E. degree in biomedical engineering (2012) from Sahand University of Technology, Tabriz, Iran and M.S. degree in biomedical engineering and got first-class honor (2015) from University of Tabriz, Tabriz, Iran.

Having published international journal papers, her research interests include fiber optic sensor design for biomedical and biomechanical applications, evolutionary optimization, and medical image processing. She currently continues her researches in the field of human musculoskeletal biomechanics in University of Tabriz.



S. Makouei received her B.Eng. degree in biomedical engineering from Sahand University of Technology, Tabriz, Iran (2005), M.S. and Ph.D. degrees in electronic engineering from Tabriz University by 2011. From 2008 to 2011, she was a member of Technical Staff at the institute of Islamic Azad University at the same time with working toward the Ph.D.

She is currently an assistant professor in the Department of Electrical and Computer Engineering in University of Tabriz and collaborates with some international journals as reviewer board member.

Having published more than twenty international journal and conference papers, her research interests include modern optical fiber design for OTDM, DWDM, FTTH, evolutionary optimization, medical image processing, and biomedical fiber optic sensors.